Utilizing Plug-in Electric Vehicles for Peak Shaving and Valley Filling in Non-residential Buildings with Solar Photovoltaic Systems

Konstantinos N. Genikomsakis[1], Benjamin Bocquier[2], Sergio Lopez[3] and Christos S. Ioakimidis[4]

[1]*DeustoTech Energy, University of Deusto, Avenida de las Universidades 24, Bilbao, Spain*
[2]*Icam Nantes, 35 Avenue du Champ de Manoeuvre, Carquefou, France*
[3]*Department of Industrial Technologies, University of Deusto, Avenida de las Universidades 24, Bilbao, Spain*
[4]*ERA Chair Holder 'Net-Zero Energy Efficiency on City Districts', Research Institute for Energy, University of Mons,*
56 Rue de l'Épargne, Mons, Belgium

Keywords: Forecasting, Non-residential Building, Peak Shaving, Photovoltaic, Plug-in Electric Vehicle, Solar Power, Valley Filling.

Abstract: This paper examines the concept of utilizing plug-in electric vehicles (PEVs) and solar photovoltaic (PV) systems in large non-residential buildings for peak shaving and valley filling the power consumption profile, given that the energy cost of commercial electricity customers typically depends on both actual consumption and peak power demand within the billing period. Specifically, it describes a hybrid approach that combines an artificial neural network (ANN) for solar irradiance forecasting with a MATLAB/Simulink model to simulate the power output of solar PV systems, as well as the development of a mathematical model to control the charging/discharging process of the PEVs. The results obtained from simulating the case of the power consumption of a university building, along with experimental parking occupancy data from a university parking lot, demonstrate the applicability and effectiveness of the proposed approach.

1 INTRODUCTION

Despite the fact that the high use of private cars, combined with low vehicle occupancy, is known to have negative impact on the quality of life and cause serious environmental and social problems (Katzev, 2003; Wolfler Calvo et al., 2004), passenger cars are still the dominant mode of transportation on land across the EU, representing some 79.9% of all passenger kilometres in 2012 (European Commission, 2014). On the one hand, with the renewed interest in electro-mobility, the reintroduction of electric vehicles (EVs) in the market has the potential to significantly reduce the environmental impact of transportation activities. On the other hand, passenger cars are largely underutilized with respect to their primary purpose. Kempton and Tomić (2005) estimate that personal vehicles are typically used for less than 5% of the time for transportation, hence plug-in electric vehicles (PEVs) are potential candidates for secondary applications in electricity markets while parked, such as provision of peak power, spinning reserves, and regulation to the grid through the vehicle-to-grid (V2G) concept. Towards the realization of the vision of the future smart grid (Güngör et al., 2011), PEVs play a key role as an energy storage resource to the grid and intelligently interact with the electric utilities (Cheng et al., 2014).

In this direction, the potential of the PEVs to serve as a dispatchable load and provide power system services, such as valley filling and peak load reduction, has received particular attention in the scientific literature (Brooks et al., 2010; Tie and Tan 2013). Indicative examples include an intelligent charging scheme for PEVs to significantly reduce the power system cost (Valentine et al., 2011), a protocol for coordinating the charging of PEVs with the electric grid (Zhang et al., 2014), as well as a strategy based on a V2G control algorithm for peak shaving and valley filling of grid power (Wang and Wang, 2013). In this regard, the large scale deployment of PEVs can leverage the penetration of renewable energy sources (RES) into the power system (Gerbelová et al., 2013; Mwasilu et al.,

179

2014).

At building level, in particular in residential or small commercial ones, the integration of RES and PEVs with capability to exchange electricity bi-directionally (i.e., charge and discharge) has been shown to allow for more efficient energy management decisions (Genikomsakis et al., 2013; Ioakimidis et al., 2014b). In this respect, forecasting of the RES output ahead of time (e.g., with a time horizon of 24 h), either in the form of solar power (Ioakimidis et al., 2013), wind power (Ioakimidis et al., 2014a; Ioakimidis et al., 2015) or both, is beneficial for the home energy management systems of the so-called electricity "prosumers", which are capable of not only consuming, but also producing and storing electricity (Grijalva and Tariq, 2011).

This paper considers the case of valley filling and peak reduction services by integrating PEVs and RES in large non-residential buildings in the context of vehicle-to-building (V2B), as a representative example of a commercial electricity customer where the energy cost depends on the actual usage (consumption), as well as on the peak power demand within the billing period. To this end, the present work combines an artificial neural network (ANN) with a MATLAB/Simulink model to forecast the output of a solar photovoltaic (PV) system and describes the development of a mathematical model for peak shaving and valley filling the consumption profile under the presence of PEVs, using as a case study the consumption characteristics of a university building, along with parking occupancy data from a university parking lot. In this context, the main contribution of this paper is to provide the integrated framework for the simulation of the system under study and the optimization of its operation, as well as to examine a number of scenarios representing different system configurations and assess the potential output by applying the proposed approach on real-world data from field measurements and consumption profiles.

2 METHODOLOGY

This section presents the methodology followed to develop the mathematical model for peak shaving and valley filling the building's consumption profile, starting from the solar irradiance forecasting model, which provides input to a MATLAB/Simulink model to simulate the output of solar PV modules.

2.1 Forecasting of Solar Irradiance

As an intermediate step of forecasting the power output of solar PV systems, the present work employs the ANN proposed by Ioakimidis et al. (2013) in order to forecast the solar irradiance for the next 24 h. The reason for considering this specific model for forecasting solar irradiance is three-fold: i) it is suitable both for sunny and cloudy days, ii) it combines forecasting accuracy with computational efficiency, and iii) it is validated with field measurement data. The key characteristic of this approach is the use of statistical feature parameters in the multilayer perceptron (MLP). The structure of the feed-forward ANN employed includes 2 hidden layers (Figure 1), with p=12 and q=16 neurons respectively, while the input vector consists of the following factors: (i) the average solar irradiance G_{Savg} in the last 24 h, (ii) the average temperature T_{avg} in the last 24 h, (iii) the maximum of the third order difference of solar irradiance TOD_{max}, (iv) the normalized discrete difference NDD between the surface and extraterrestrial irradiance, and (v) the day of the year d. The output layer is a vector of 24 components representing the forecasted solar irradiance for the next 24 h.

The datasets for training the ANN are normalized in the interval [-1,1] using equation (1), where y_{min} equals -1, y_{max} equals 1, while x_{max} and x_{min} are the maximum and minimum values in each dataset.

$$y = y_{min} + \frac{(y_{max} - y_{min})(x - x_{min})}{(x_{max} - x_{min})} \quad (1)$$
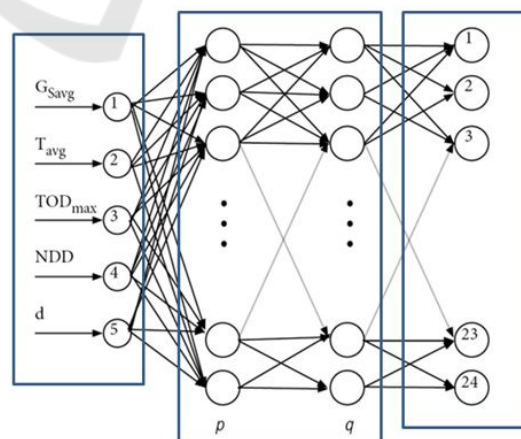

Figure 1: Structure of the ANN-based model for solar irradiance forecasting.

The forecast of solar irradiance for a period of 6

days (using a resolution of 24 hourly values) in the area under study in Bilbao, Spain, is illustrated in Figure 2.

2.2 Simulation Model of PV Output

For the purposes of this work, the simulation of the solar PV output is based on the model proposed by Pandiarajan and Muthu (2011). More specifically, a PV cell is represented with the equivalent electrical circuit in Figure 3, thus its output current I is given in equation (2).

$$I = I_{ph} - I_d - I_{sh} \quad (2)$$

where I_{ph} is the cell photocurrent, I_d is the diode current and I_{sh} is the shunt current. The relation between the cell parameters, output current I and output voltage V is expressed in the characteristic equation (3).

$$I = I_{ph} - I_0 \left\{ \exp \left[\frac{q(V + IR_s)}{nkT} \right] - 1 \right\} - \frac{V + IR_s}{R_{sh}} \quad (3)$$

where I_0 is the reverse saturation current, q is the elementary charge, R_s is the series resistance, n is the diode ideality factor, k is the Boltzmann's constant, T is the absolute temperature, and R_{sh} is the shunt resistance.

PV cells are combined together to form PV modules, while the latter are inter-connected in larger assemblies to form PV panels. In this work, the model that describes the operation of an assembly of N_p cells in parallel and N_s cells in series is mathematically expressed in equations (4)-(7).

Specifically, equation (4) expresses the module photocurrent I_{PH}:

$$I_{PH} = \left[I_{SCr} + K_i(T - 298) \right] \frac{\lambda}{1000} \quad (4)$$

where I_{SCr} is the PV module short-circuit current (at 25 °C and 1000 W/m^2), K_i is the short-circuit current temperature co-efficient at I_{SCr}, and λ is the PV module illumination.

Equation (5) expresses the module reverse saturation current I_{RS}:

$$I_{RS} = \frac{I_{SCr}}{\exp\left(\frac{qV_{oc}}{N_s kAT}\right) - 1} \quad (5)$$

where V_{oc} is the open-circuit voltage and A is an ideality factor.
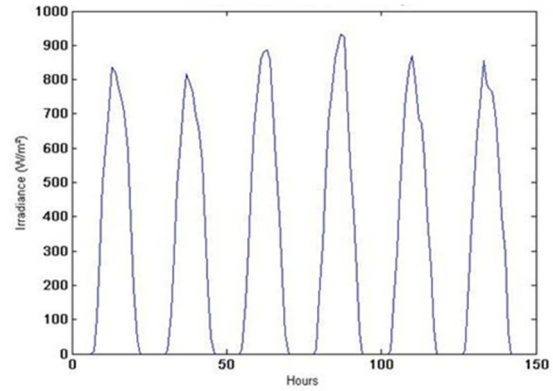

Figure 2: Example output of forecasted solar irradiance with the ANN-based model.
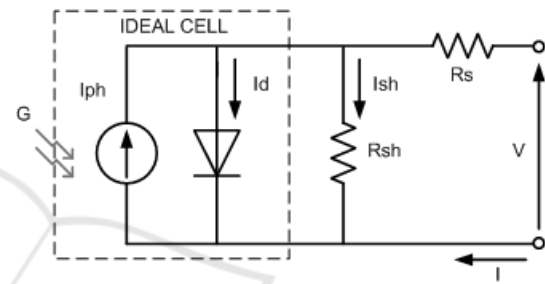

Figure 3: Equivalent circuit of a PV cell.

Equation (6) expresses the module saturation current I_0:

$$I_0 = I_{RS} \left(\frac{T}{T_r}\right)^3 \exp\left[\frac{qE_{g0}}{Bk}\left(\frac{1}{T_r} - \frac{1}{T} \right) \right] \quad (6)$$

where E_{g0} is the band gap for silicon (= 1.1 eV), T_r is the reference temperature (= 298 °K), and B is an ideality factor.

The module output current I_{PV} is given in equation (7):

$$I_{PV} = N_P I_{PH} - N_P I_0 \left\{ \exp\left[\frac{q(V_{PV} + I_{PV}R_S)}{N_S AkT} \right] - 1 \right\} \quad (7)$$

where V_{PV} is the output voltage and R_S is the series resistance of the PV module.

The aforementioned equations that describe the operation of a PV module were modelled in MATLAB/Simulink, as proposed by Pandiarajan and Muthu (2011), with basic modifications to adapt the model according to the specifications and requirements of the present work. Indicatively, Figure 4 illustrates the high-level representation of a PV system model in MATLAB/Simulink, while Figure 5 shows the output power of a single PV module with $N_P = 1$ cell and $N_S = 50$ cells.
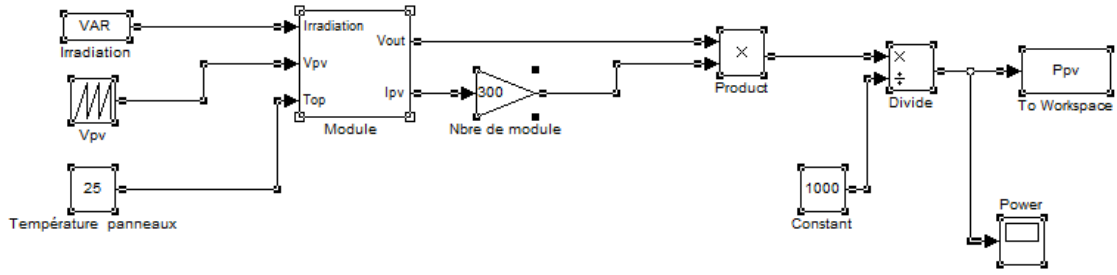
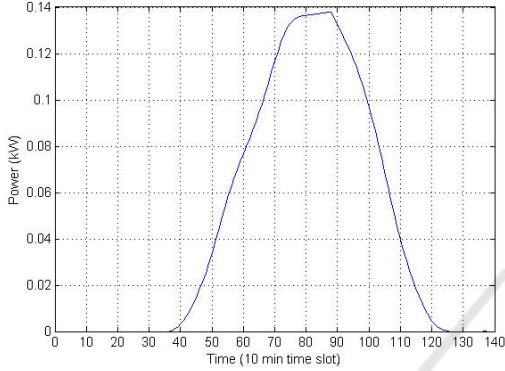Figure 4: Model of PV system in MATLAB/Simulink.

Figure 5: Power output of 1 PV module.

2.3 Mathematical Model for Peak Shaving and Valley Filling of Power Consumption using PEVs

This subsection considers the charging and discharging process of PEVs for a period of 1 day, divided evenly in N intervals, based on the approach proposed by He et al. (2012). The interval length τ is chosen equal to 10 min, while the charging or discharging power in each interval i is assumed to be constant. Let also m denote a vehicle in the set of vehicles M charging and discharging over the day.

By convention, it is assumed that the charging or discharging power x_{mi}, for each $m \in M$ and $i \in N$, is negative during discharging and positive during charging of the PEV battery. Assuming a slow charging process, the constraint imposed by the charging station on the maximum charging or discharging power p_{max} is expressed in (8).

$$-p_{\max} \leq x_{mi} \leq p_{\max}, \quad \forall m \in M \tag{8}$$

A PEV m may charge and discharge during a period T_m, defined by the time of arrival t_m^{arr} and time of departure t_m^{dep} to/from the parking lot of the building. To this end, the presence of the PEV is denoted by f_{mi} as defined in equation (9).

$$f_{mi} = \begin{cases} 1 & \text{if interval } i \text{ is in period } T_m \\ 0 & \text{otherwise} \end{cases} \tag{9}$$

Let y_i be the load of charging/discharging the PEVs in interval i, as given in equation (10).

$$y_i = \sum_{m \in M} x_{mi} f_{mi} \tag{10}$$

Moreover, let E_m^{ini} be the initial energy of the PEV battery, E_m^{cap} be its capacity (assumed equal to 24 kWh), and E_{Tm+1} be the battery energy required for the next trip of the PEV (assumed to be provided by the user of the vehicle). The final energy of the PEV battery E_m^{fin} at the end of the charging period T_m is expressed in (11).

$$E_m^{fin} = E_m^{ini} + \sum_{i \in N} \tau x_{mi} f_{mi} \geq E_{T_{m+1}}, \forall m \in M, \forall i \in N \tag{11}$$

In addition, the lower and upper bounds of the energy during the charging/discharging process of the PEV battery are expressed in (12), i.e. the battery energy cannot be less than 0 and cannot exceed its capacity (He et al., 2012), where $Q(i)$ denotes the set of intervals prior to interval i.

$$0 \leq E_m^{ini} + \sum_{k \in Q(i)} \tau x_{mk} f_{mk} \leq E_m^{cap}, \forall m \in M, \forall i \in N \tag{12}$$

The constraint in (13) specifies that the energy charged to the PEV battery at the end of the period T_m is at least equal to that discharged from the battery during T_m, while the constraint in (14) ensures that the energy exchange takes place only when PEVs are present (parked).

$$\sum_{i \in N} \tau x_{mi} f_{mi} \geq 0, \forall m \in M \tag{13}$$

$$x_{mi} \overline{f_{mi}} = 0, \quad \forall m \in M, \forall i \in N \tag{14}$$

where $\overline{f_{mi}}$ is the binary complement of f_{mi}.

Furthermore, it is assumed that Pu_i denotes the power consumption of the building in the interval i, and C is the constant defined in equation (15).

$$C = \left[\max(Pu_i) + \min(Pu_i)\right] / 2 \qquad (15)$$

Mathematically, the objective of peak shaving and valley filling the curve of the building's power consumption, while taking into the load y_i from the charging/discharging process of the PEVs and the power output Ppv_i from the PV system in each interval i, is formulated in (16). For the purposes of this work, this optimization problem is solved in MATLAB using the *fmincon* solver.

$$\text{Minimize } z = \sum_{i \in N}(Pu_i + y_i - Ppv_i - C)^2 \qquad (16)$$

3 SIMULATION AND RESULTS

As a case study, the present work considers the power consumption curve of a building at the campus of University of Deusto, Spain. The aim is to simulate the impact of controlling the charging/discharging process of (potentially parked) PEVs in order to flatten the power consumption curve, as shown in Figure 6, by taking into account real-world profiles of parking occupancy from conventional cars at a university parking lot.

3.1 Simulation Setting and Scenarios

The developed model is employed to examine six scenarios for different number of PEVs and PV modules. Table 1 shows the configuration of the six scenarios under study.

The required data for the parking occupancy of PEVs were obtained from a field experiment, where a team of participants recorded the parking spot (place) and time of (conventional) cars at a specific parking lot of the university campus, having a capacity of 65 cars (Genikomsakis et al., 2015). Indicatively, the occupancy of the 8 (randomly chosen) parking spots employed for scenarios 1 and 2 is illustrated in Figure 7, where the colored bars denote the time of presence of the different vehicles (horizontal axis) at each parking spot (vertical axis).

3.2 Simulation Results

The simulations were carried out in MATLAB on the basis of the scenarios defined in the previous subsection. As already pointed out, it is assumed that the PEVs can discharge their battery to provide power to the building and reduce its power consumption, whereas they add extra load to the power consumption of the building when they

charge their battery. Figures 8 and 9 illustrate the obtained results of the scenarios 1 and 2 respectively.
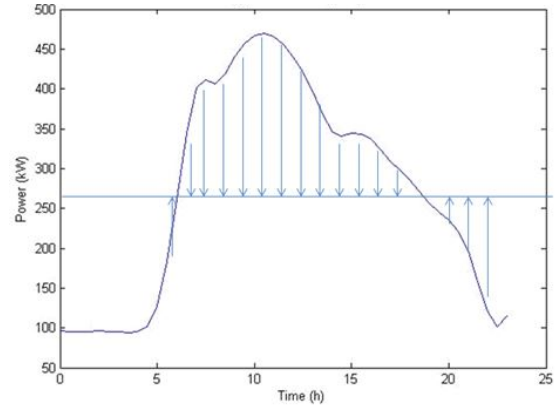

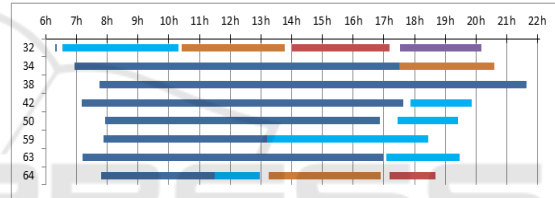Figure 6: Power consumption curve of the building under study for a typical winter day.

Figure 7: Occupancy of 8 randomly chosen parking spots.

Table 1: Overview of the six simulated scenarios.

Scenario	Number of parking spots	Number of PV modules
1	8	300
2	8	600
3	35	300
4	35	600
5	65	300
6	65	600

As a first observation, the results of scenarios 1 and 2 indicate that the impact of the available PEVs at the 8 parking spots on the power consumption curve of the building is rather low. Nevertheless, there is a more pronounced effect when considering both the contribution of PEVs and the PV production. As expected, the contribution of the PV system becomes higher during midday hours when the PV production reaches its peak.

Figure 9 shows that the power consumption curve of the building is peak shaved between 7:00 am and 12:00 pm. After this period, the charging of PEVs causes the red curve representing the final power consumption to cross the green curve representing the building power consumption minus

the photovoltaic power production. Moreover, the final power consumption curve does not cross the initial power consumption curve (in blue color) until 6:30 pm, indicating that the PV production is enough to cover the charging of the PEVs for this period. At the end of the day, after 6:30 pm, the final consumption is slightly higher or equal to the initial consumption.

Figures 10 and 11 illustrate the results obtained for scenarios 3 and 4, where the number of available parking spots for charging/discharging the PEVs amounts to 35, while the number of simulated PV modules is 300 and 600 units respectively. The

increase of the available PEVs flattens the power consumption curve of the building, approaching the target constant as a result of the improved valley filling and peak shaving. The majority of the PEVs discharge at peak power consumption and charge when the building's power consumption is at lower levels.

When the PV production is doubled (Figure 11), the valley filling effect becomes more intense. Moreover, the effect of lowering the power consumption curve of the building takes place mostly between noon and 3:00 pm (compared to scenario 3), where the PV production is at its highest
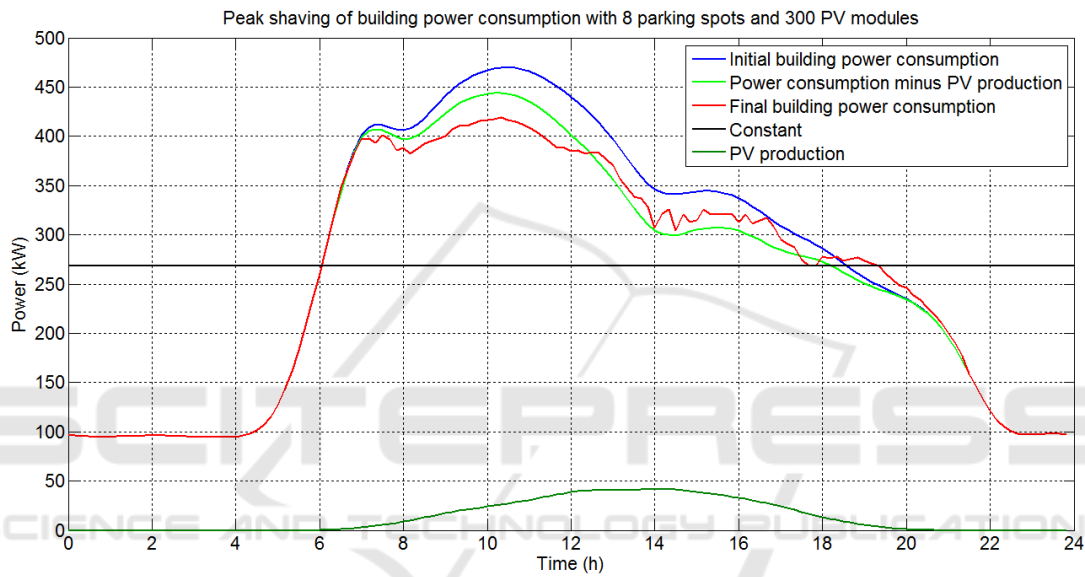

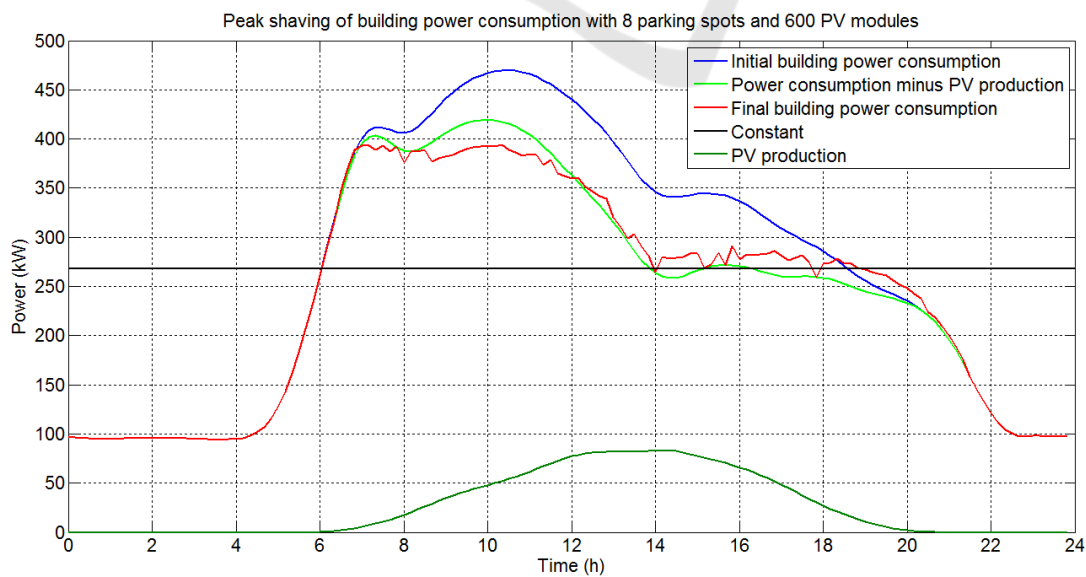Figure 8: Scenario 1 results.
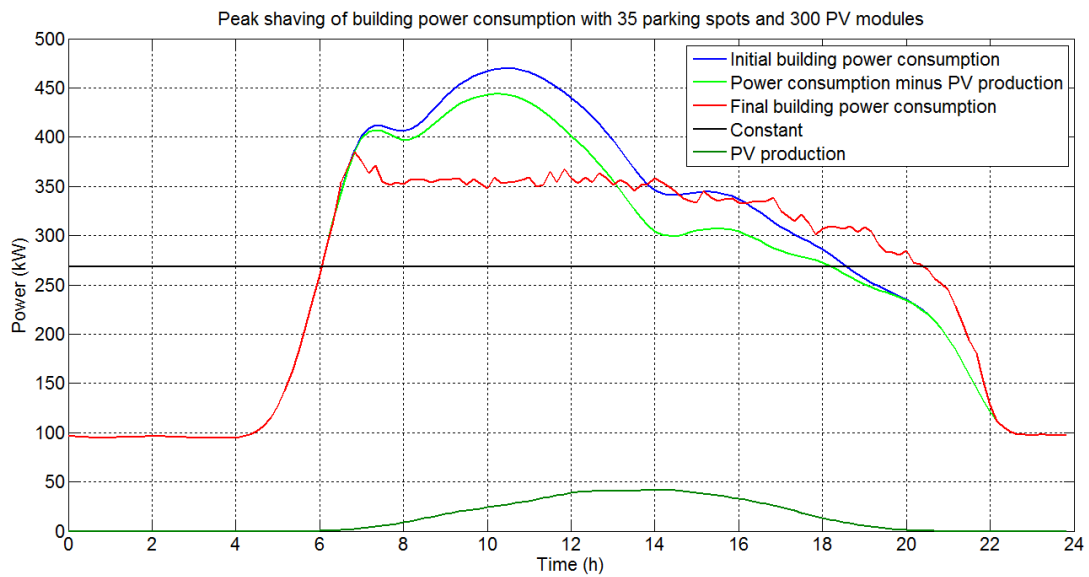

Figure 9: Scenario 2 results.
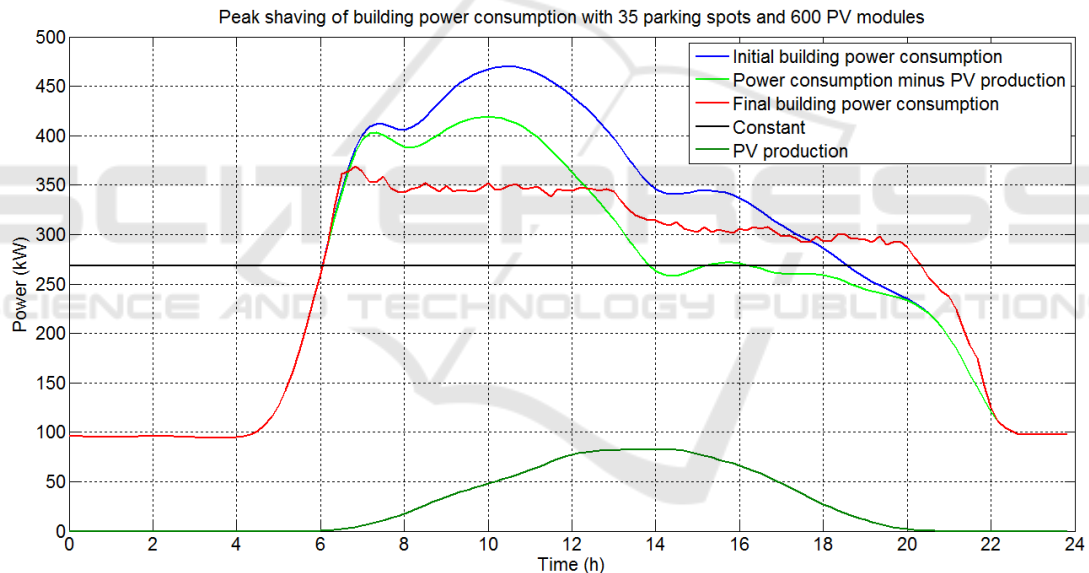
Figure 10: Scenario 3 results.

Figure 11: Scenario 4 results.

level. The roughness of the final consumption curve is mainly due to the randomness of the charging/discharging process of the PEVs.

The results of scenarios 5 and 6 are depicted in Figures 12 and 13. Specifically, the last two scenarios consider 65 available parking spots for charging/discharging of PEVs. In both cases, the results reveal that the number of PEVs is high enough to regulate by themselves the power consumption of the building, with the PV production contributing to a lesser extent to the smoothing of the final consumption curve. It is obvious that in

scenarios 5 and 6, the final curve of the building consumption is almost flat, resulting in effective peak shaving and valley filling. In particular, it remains almost at the same level from 6:00 am until 8:00 pm by shifting the charging of the PEVs, more notably after 4:00 pm, where the initial power consumption curve of the building would decrease further.

In Figure 13, which illustrates the simulation results for the last scenario considering 600 PV modules, the pattern of the final consumption curve presents no significant changes (compared to

scenario 5), despite the fact that the increased PV production reduces further the final power consumption.

Table 2 summarizes the main findings of this work. As expected, the highest peak shaving occurs under scenario 6. The high number of available

PEVs at the 65 parking spots in combination with the high additional energy contribution of the 600 PV modules, offers enough flexibility to the system resulting in more than 25% peak shaving compared to the initial power consumption of the building. In addition, it is noted that the power gap with the
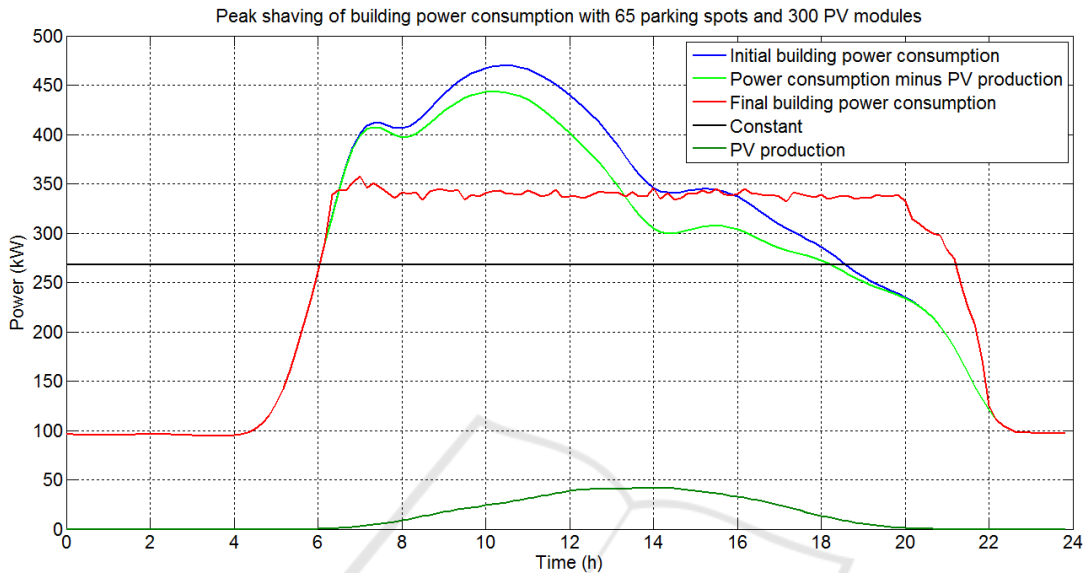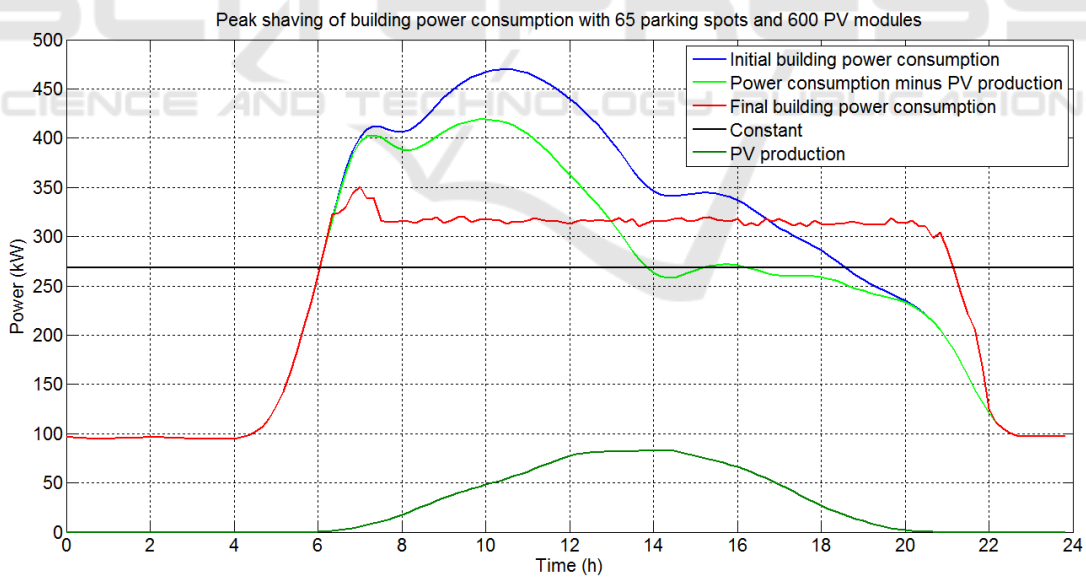

Figure 12: Scenario 5 results.

Figure 13: Scenario 6 results.

Table 2: Comparative simulation results.

Parking spots	8	8	35	35	65	65
PV modules	300	600	300	600	300	600
Final peak consumption (kW)	420	395	380	370	355	350
Decrease compared to initial peak (%)	10.1	15.4	18.6	20.8	24.0	25.1
Gap with constant C (kW)	152	127	112	102	87	82

reference flat consumption, i.e. constant *C*, becomes smaller as the number of available PEVs and PV modules increases.

4 CONCLUSIONS

This paper examines the impact of PEVs and PV production as a means of providing peak shaving and valley filling services in the context of V2B. More specifically, it employs the profiles of power consumption and parking occupancy from a building and a parking lot at University of Deusto, Spain, in order to provide the required input to the proposed model and simulate a number of scenarios for the envisaged system.

To this end, the present paper initially described the integration of an ANN-based solar irradiance forecasting model with a MATLAB/Simulink model to simulate the output of solar PV modules. Next, a mathematical model was developed and solved in MATLAB in order to examine and quantitatively analyze the impact of connected PEVs and PV production on the power consumption of the building.

As confirmed also by the simulation results, the higher the number of available PEVs and PV modules, the closer the achievable load curve of the building comes to the target (flat) curve. On the one hand, the results demonstrate the feasibility of the peak shaving and valley filling approach proposed in this paper, and on the other hand, they highlight the importance of the number of connected vehicles on its effectiveness.

As a concluding remark, it is noted that this work employed a deterministic approach to model the consumption of the building, the presence of PEVs at the parking lot and the energy of their battery both in the initial and final state. Hence, directions for future work include incorporating the uncertainties in the arrival and parking duration of the PEVs, the initial and final energy of their battery, as well as the consumption profile of the building.

REFERENCES

Brooks, A., Lu, E., Reicher, D., Spirakis, C., Weihl, B., 2010. Demand dispatch. *IEEE Power and Energy Magazine* 8(3), pp. 20-29.

Cheng, X., Hu, X., Yang, L., Husain, I., Inoue, K., Krein, P., Lefevre, R., Li, Y., Nishi, H., Taiber, J.G., Wang, F.-Y., Zha, Y., Gao, W., Li, Z., 2014. Electrified vehicles and the smart grid: The ITS perspective.

IEEE Transactions on Intelligent Transportation Systems 15(4), pp. 1388-1404.

European Commission, 2014. EU transport in figures: Statistical Pocketbook 2014, pp. 1-138.

Genikomsakis, K. N., Angulo Gutierrez, I., Thomas, D., and Ioakimidis, C.S., 2015. Simulation and Design of a Fast Charging Battery Station in a Parking Lot of an e-Carsharing System. In *Proceedings of the 4th International Conference on Renewable Energy Research and Applications, ICRERA 2015*.

Genikomsakis, K. N., Ioakimidis, C. S., Eliasstam, H., Weingraber, R., Simic, D., 2013. A non-myopic approach for a domotic battery management system. In *Proceedings of the 39th Annual Conference of the IEEE Industrial Electronics Society, IECON 2013*, pp. 4522-4527.

Gerbelová, H., Genikomsakis, K. N., Ioakimidis, C. S., 2013. Electric vehicles charging under a G2V and V2G approach: The case of the portuguese power system. In *Proceedings of the 26th International Conference on Efficiency, Cost, Optimization, Simulation and Environmental Impact of Energy Systems, ECOS 2013*.

Grijalva, S., Tariq, M. U., 2011. Prosumer-based smart grid architecture enables a flat, sustainable electricity industry. *IEEE PES Innovative Smart Grid Technologies Conference Europe, ISGT Europe*.

Güngör, V. C., Sahin, D., Kocak, T., Ergüt, S., Buccella, C., Cecati, C., Hancke, G.P., 2011. Smart grid technologies: Communication technologies and standards. *IEEE Transactions on Industrial Informatics* 7(4), pp. 529-539.

He, Y., Venkatesh, B., Guan, L., 2012. Optimal scheduling for charging and discharging of electric vehicles. *IEEE Transactions on Smart Grid* 3(3), pp. 1095-1105.

Ioakimidis, C. S., Genikomsakis, K. N., Dallas, P. I., Lopez, S., 2015. Short-term wind speed forecasting model based on ANN with statistical feature parameters. In *Proceedings of the 41st Annual Conference of the IEEE Industrial Electronics Society, IECON 2015*, pp. 971-976.

Ioakimidis, C. S., Lopez, S., Genikomsakis, K. N., Rycerski, P., Simic, D., 2013. Solar production forecasting based on irradiance forecasting using artificial neural networks. In *Proceedings of the 39th Annual Conference of the IEEE Industrial Electronics Society, IECON 2013*, pp. 8121-8126.

Ioakimidis, C. S., Oliveira, L. J., Genikomsakis, K. N., 2014a. Wind power forecasting in a residential location as part of the energy box management decision tool. *IEEE Transactions on Industrial Informatics* 10(4), pp. 2103-2111.

Ioakimidis, C. S., Oliveira, L. J., Genikomsakis, K. N., Dallas, P. I., 2014b. Design, architecture and implementation of a residential energy box management tool in a SmartGrid. *Energy* 75, pp. 167-181.

Katzev, R., 2003. Car Sharing: A New Approach to Urban Transportation Problems. *Analyses of Social Issues*

and Public Policy 3(1), pp. 65-86.

Kempton, W., Tomić, J., 2005. Vehicle-to-grid power fundamentals: Calculating capacity and net revenue. *Journal of Power Sources* 144(1), pp. 268-279.

Mwasilu, F., Justo, J. J., Kim, E.-K., Do, T. D., Jung, J.-W., 2014. Electric vehicles and smart grid interaction: A review on vehicle to grid and renewable energy sources integration. *Renewable and Sustainable Energy Reviews* 34, pp. 501-516.

Pandiarajan, N., Muthu, R., 2011. Mathematical modeling of photovoltaic module with Simulink. In *Proceedings of the 2011 1st International Conference on Electrical Energy Systems, ICEES 2011*, pp. 258-263.

Tie, S. F., Tan, C. W., 2013. A review of energy sources and energy management system in electric vehicles. *Renewable and Sustainable Energy Reviews* 20, pp. 82-102.

Valentine, K., Temple, W. G., Zhang, K. M., 2011. Intelligent electric vehicle charging: Rethinking the valley-fill. *Journal of Power Sources* 196(24), pp. 10717-10726.

Wang, Z., Wang, S., 2013. Grid power peak shaving and valley filling using vehicle-to-grid systems. *IEEE Transactions on Power Delivery* 28(3), pp. 1822-1829.

Wolfler Calvo, R., de Luigi, F., Haastrup, P., Maniezzo, V., 2004. A distributed geographic information system for the daily car pooling problem. *Computers and Operations Research* 31(13), pp. 2263-2278.

Zhang, L., Jabbari, F., Brown, T., Samuelsen, S., 2014. Coordinating plug-in electric vehicle charging with electric grid: Valley filling and target load following. *Journal of Power Sources* 267, pp. 584-597.